JOURNAL OF NANO- AND ELECTRONIC PHYSICS
Vol. **6** No 2, 02022(7pp) (2014)

ЖУРНАЛ НАНО- ТА ЕЛЕКТРОННОЇ ФІЗИКИ
Том **6** № 2, 02022(7cc) (2014)

The Phase Composition and Magnetic Properties of Film Systems Based on Fe(Co) and Gd(Dy)

S.I. Vorobiov[1], I.V Cheshko[1], A.M. Chornous[1], H. Shirzadfar[2], O.V. Shutylieva[1]

[1] *Sumy State University, 2, Rimsky Korsakov Str., 40007 Sumy, Ukraine*
[2] *Institut Jean Lamour, UMR CNRS 7198, Université de Lorraine, 54506 Vandœuvre-lès-Nancy, France*

(Received 31 March 2014; revised manuscript received 03 June 2014; published online 20 June 2014)

The article represents the results of a comprehensive study of the structural and phase state and magnetic properties of three-layer Co(Fe)/Gd(Dy)/Co(Fe)/Sub film systems before and after heat treatment. It is shown that the structural and phase state of Gd and Dy films depends on their thickness, and the processes of phase formation in three-layer films have a number of features. It is established that magnetic properties of film systems correlate with their structural and phase state, leading to a change in the coercive force and residual magnetization and the nature of the dependences between the film magnetization and the applied external magnetic field.

Keywords: Thin films, Rare earth metals, Magnetic hysteresis, Phase composition, Residual magnetization, Coercive force.

PACS numbers: 68.55.Nq, 71.20.Be, 71.20.Eh, 75.60.Ej

1. INTRODUCTION

Combination of nanoscale layers based on rare-earth (R) and transition (T) metals has prospects of wide application in the production of new device structures [1] that is due to the features of mutual antiferromagnetic ordering in the R/T systems. It can be realized during the stabilization of amorphous (quasi-amorphous) state in the layers of R metals and observance of certain formation conditions and parameters of the film samples. High Values of the magnetic characteristics can be obtained in such systems, but stability of the working parameters of elements is determined at some combination of the components and by their structural and phase state.

Generally [2-4], magnetic properties of nanoscale film systems based on R/T metals with Fe (Co) and Gd (Dy) layers are investigated in the composition of more complicated multilayer functional film systems (see, for example, [2]). There are works [3, 4], in which temperature effects in magnetic characteristics of $[Gd / Fe]_n$ multilayers have been studied. Investigations, where film systems based on Gd and Fe, Co and Dy have been considered as independent functional elements, are less common. The authors of the works [5, 6] present the investigation results of the phase composition and tenso-resistive properties of multilayer film materials based on Fe and rare-earth [5] or noble [6] metals as sensitive elements of strain sensors. The authors of the work [7] have shown the possibility of the observation of the giant magnetoresistance effect in Gd/Fe system even at room temperature. But in all the cases the key objective of the works was to investigate the properties of the mentioned film structures based on R/T metals only with partial analysis of their structural features and phase composition.

Thus, establishment of the formation conditions of the structurally unordered Gd and Dy phases and their stability in the composition of multilayer film systems Fe(Co)/Gd(Dy)/Fe(Co)/Sub (Sub is the substrate) defines the purpose of the given work, which can be reached only using a comprehensive approach to the study of the structural and phase state and magnetic properties.

2. EXPERIMENTAL TECHNIQUE

We have obtained and investigated the sets of the samples of the Fe/Gd/Fe, Co/Gd/Co and Co/Dy/Co film systems, in which thicknesses of separate layers (below in the brackets they are given in nm) had the following values: T(5)/R(1-20)/T(20)/Sub. Some film systems of each set were obtained in one technological cycle by the method of electron-beam deposition at such condensation conditions as:
– residual gas pressure $P \cong 10^{-4}$ Pa;
– substrate temperature $T_s \cong 460$ K;
– substrate type: glass ceramics for the investigation of the magnetic properties and amorphous carbon – for the diffraction study;
– average condensation rate $\omega = 0.01 – 0.03$ nm/s.

Thickness of the samples during condensation was determined using quartz resonator. Substrate temperature was controlled by chromel-alumel thermocouple.

Thermal treatment of the samples was carried out by the scheme "heating → ageing during 15 min at T_a → cooling to room temperature". Annealing temperature for the Co/Gd(Dy)/Co and Fe/Gd/Fe systems was, respectively, equal to $T_a = 800$ and 1000 K and $T_a = 700$ and 900 K. Electron microscope PEM-125K was used for the investigation of the phase composition.

Study of the magnetic properties was performed by the method of vibrating magnetometry at room temperature using the device VSM Lake Shore 7400. Measurements were carried out at the parallel measurement geometry (magnetic flux lines were directed parallel to the sample surface). Sample on a holder of quartz glass was rotated around the axis which coincided with the normal to the surface.

As a result, we have obtained the dependences of the magnetization on the external magnetic field strength that allowed to plot the hysteresis loops for each individual case. Using the intercept on the abscissa axis we have found the coercive force (H_c) and by the intercept on the ordinate axis we have determined the residual magnetization (M_r).

3. RESULTS OF THE EXPERIMENTAL INVESTIGATIONS

3.1 Phase formation processes

According to the literature data, as-deposited single-layer films of Gd [5] and Dy [6] rare-earth metals are inclined to amorphization. And, as it was shown in [9], the degree of disorder of their structures strongly depends on the film thickness and substrate temperature during condensation. A quasi-amorphous phase is observed on the electron diffraction patterns for the effective thicknesses of Gd layers less than 10 nm, and with the increase in the thickness the crystallization processes are manifested.

Analysis of the results of the electron diffraction investigations (Fig. 1) implies that Gd films of the thickness from 10 nm to 40 nm in as-deposited state have the hcp-Gd + fcc-GdH_2 phase composition with traces of the bcc-Gd_2O_3 which are present in the samples of the thickness of $d < 20$ nm (Fig. 1a).

In accordance with the state diagram [10], formation of hydrides GdH_2 with the cubic structure and lattice parameter $a_0 = 0.530$ nm and GdH_3 with the hexagonal structure ($a_0 = 0.373$ nm and $c_0 = 0.671$ nm) is possible in the Gd-H system. The majority of interplanar spacings of fcc-GdH_2 and hcp-Gd are very close in values and this leads to the overlap of lines on the electron diffraction patterns and complication of their unambiguous interpretation. However, some reflections from crystallographic planes, such as (311) and (331), are interpreted unambiguously as those which belong to the phase of GdH_2 hydride. The data we have obtained implies that the average lattice parameter of the fcc-phase is equal to $a_{av} = 0.528$ nm that is slightly less than the tabulated value a_0 for GdH_2. Such result is probably connected with depletion of GdH_2 lattice by hydrogen atoms, and fcc-phase should be interpreted as GdH_x, where $x \approx 2$, but for simplification we will further use the notation GdH_2.

In a bulk state gadolinium and oxygen form Gd_2O_3 oxide of three different modifications A, B and C [10]. The latter represents the bcc-Gd_2O_3 with the lattice parameter $a_0 = 1.081$ nm. Two other phases pass into one another at temperatures higher than 1400 K and are considered high temperature [10]. On the electron diffraction patterns (Fig. 1a) from single-layer Gd films one can observe lines corresponding to the reflections from bcc-Gd_2O_3 crystallographic planes. (211), (332) and (134) are the characteristic lines of the oxide which do not coincide with lines from other phases. Intensity of these lines on the electron diffraction patterns for unannealed samples is relatively low; therefore, one can talk only about the traces of Gd_2O_3 which became the result of the oxide formation during the investigations. To judge by the increase in the line intensity on the electron diffraction patterns from the corresponding Gd film samples (see Fig. 1d) relative to those, which were not thermally treated (Fig. 1a), one can conclude as follows: content of the oxide phase in the thermally annealed samples increases due to the interaction with oxygen atoms of residual atmosphere. Stabilization of the oxide phase can be also observed on the corresponding micrographs of the crystal structure of monolayer Gd films (Fig. 1d) in the form of dark inclusions with typical round shape of the average size to 50 nm.

We have to note that study of the phase composition of Gd films without protective coating is considerably complicated by its high chemical activity. And, even, the samples obtained in rather pure vacuum conditions in further investigations, for example, by the methods of

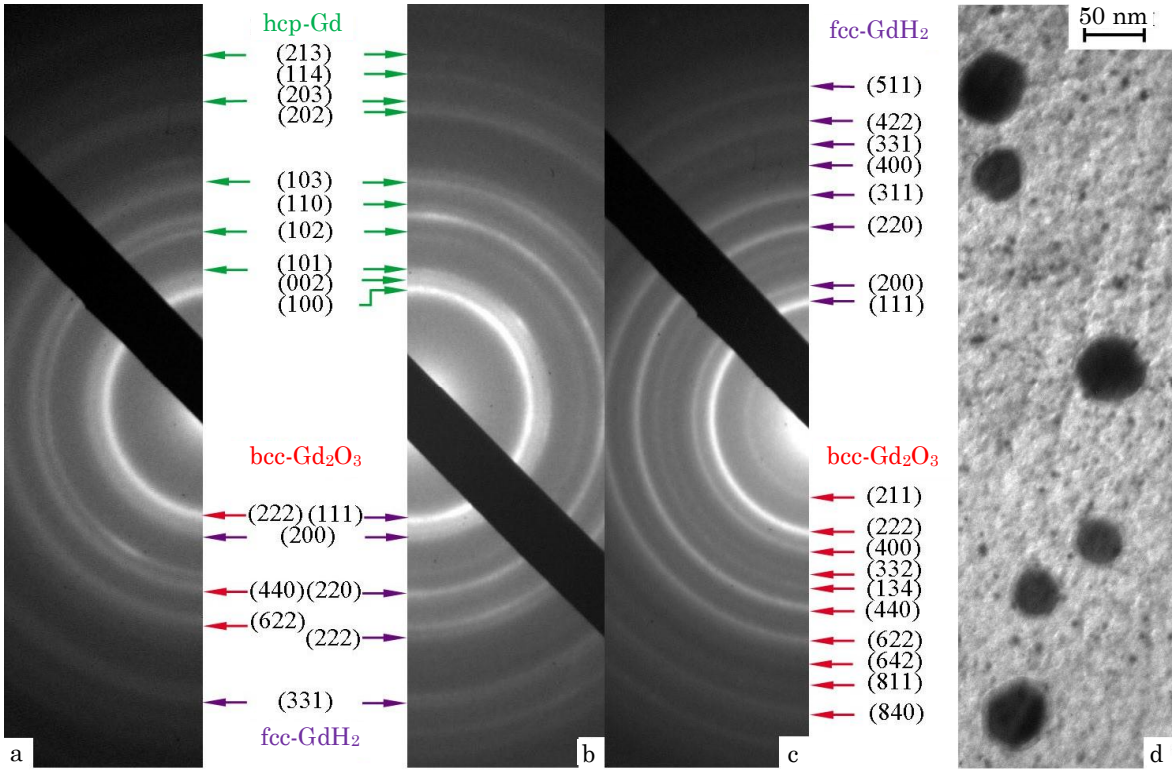

Fig. 1 – Electron diffraction patterns from monolayer Gd films in the as-deposited state: a – Gd(15)/Sub; b – Gd(35)/Sub and after thermal treatment to $T_a = 700$ K: c – Gd(15)/Sub and its microstructure (d)

the transmission electron or atomic-force microscopy are impossible without partial oxidation of the film samples. This should be taken into account during the analysis of the obtained results.

The main difference of the phase composition of Dy films consists in the absence there of hydride phases both in as-deposited state and after all stages of further thermal treatment (Fig. 2). But oxidation processes are manifested in these films. Depending on the film thickness, characteristic lines (222) and (400) of the bcc-Dy_2O_3 of different intensity are fixed on the electron diffraction patterns along with the hcp-Dy lines. Average value of the lattice parameters is equal to $a_{av} = 0.358$ nm, $c_{av} = 0.566$ nm ($a_0 = 0.359$ nm and $c_0 = 0.5647$ nm [11]) for the hcp-Dy and $a_{av} = 1.07$ nm ($a_0 = 1.066$ nm [11]) for the bcc-Dy_2O_3.

We have presented earlier in the works [12, 13] the investigation results of the features of the structural characteristics and phase state of monolayer Co and Fe films. We should only note that Fe films in the whole thickness range have the bcc-phase with the lattice parameter before annealing $a_{av} = 0.284$ nm, which slightly increases after annealing at $T_a = 700$ K to the value of $a_{av} = 0.285$ nm ($a_0 = 0.286$ [14]) due to the ordering of the crystal structure of grains. For Fe films, which were thermally treated at higher temperatures, depending on their thickness, the impurity fcc-Fe_3 phase is fixed along with the bcc-Fe on the electron diffraction patterns.

Monolayer Co films after condensation are stabilized to the hcp-phase, although two lines (111) and (200), which belong to the reflections from the fcc-Co crystallographic planes, are observed on the electron diffraction patterns. This is due to the presence in the hcp-phase of stacking faults [15, 16]. In Co samples after thermal treatment to the temperatures of $T_a = 800$ and 1000 K intensity of the lines, which correspond to the fcc-Co, considerably increases, although reflections from the hcp-Co crystallographic planes are fixed on the electron diffraction patterns but with lower intensity. Thus, monolayer Co films have phase composition hcp-Co + fcc-Co with the lattice parameters in the annealed state of the fcc-Co – $a = 0.356$ nm ($a_0 = 0.3545$ nm [12]) and the hcp-Co – $a = 0.253$ nm and $c = 0.412$ nm ($a_0 = 0.2514$ nm and $c_0 = 0.4105$ [14]).

Going to the multilayer film systems based on R/T metals, phase composition of Co and Fe layers in as-deposited state and after thermal treatment corresponds to the phase composition of monolayer films of these metals (Fig. 3). At the same time, phase formation processes in the layers of rare-earth metals have a number of features. Thus, in the case of three-layer films based on Co and Fe and Gd with the thickness of the latter of 10-25 nm, formation of the fcc-GdH_2 only takes place in as-deposited state. This phase also remains after thermal treatment to the temperature of 1000 K, although in some cases traces of the bcc-Gd_2O_3 oxide phase are fixed on the electron diffraction patterns. For the film system Co/Dy/Co/Sub with the thickness of Dy sublayer from 10 to 25 nm, the hcp-Dy and bcc-Dy_2O_3 phases are fixed on the electron diffraction patterns both in as-deposited state and after thermal treatment to the temperatures of $T_a = 800$ and 1000 K that also took place in the monolayer Dy films. For the film systems based on the considered R/T metals in the case when effective layer thickness of rare-earth metal is less than 10 nm, they, as well as the monolayer films of these metals, have phase composition corresponding to the quasi-amorphous Gd and Dy.

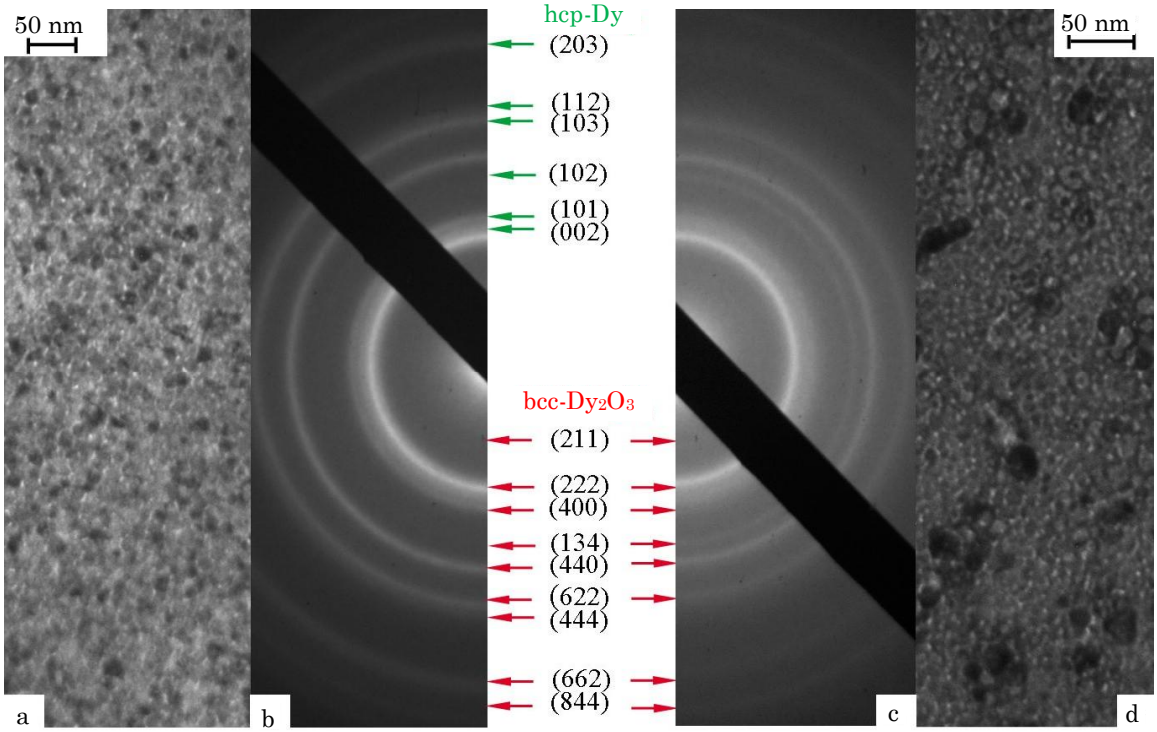

Fig. 2 – Electron diffraction patterns from monolayer Dy(25)/Sub films and their microstructure in as-deposited state (a, b) and after thermal treatment to $T_a = 700$ K (c, d)

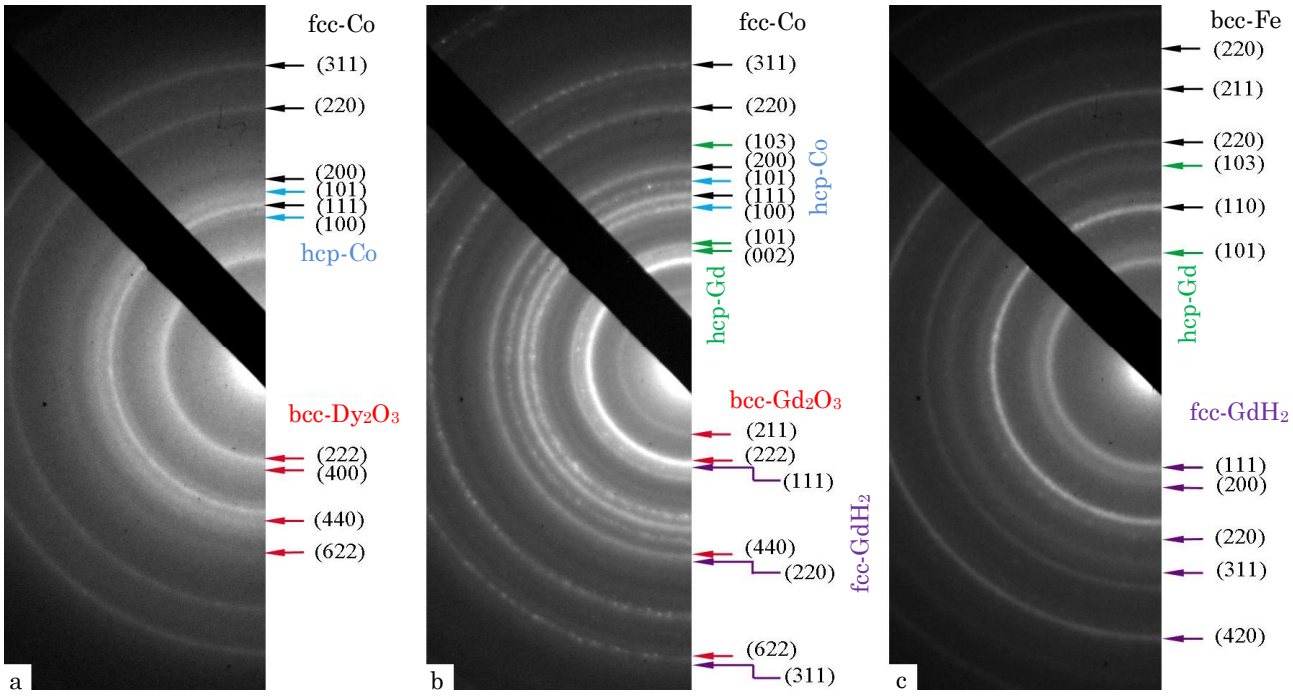

Fig. 3 – Electron diffraction patterns from three-layer films: Co(5)/Dy(15)/Co(20)/Sub (a), Co(5)/Gd(25)/Co(20)/Sub (b) and Fe(5)/Gd(20)/Fe(20)/Sub (c) after thermal treatment to T_a = 800, 1000 and 700 K, respectively

3.2 Magnetic properties

3.2.1 Monolayer Co and Fe films

The feature of our investigation of the magnetic properties of single-layer Co and Fe films relative to those specified in the literature (see, for example, [12, 17]) consists in the comprehensive study of the dimensional dependence of such important magnetic characteristics as the residual magnetization M_r and coercivity H_c and determination of the influence on them of the structural and phase state of the films before and after thermal annealing. But the main task of this investigation was to obtain the data about monolayer films which were the components of three-layer films based on R/T metals. We should note that mono- and three-layer films were produced and thermally treated under the same technological conditions. This will allow in the sequel to determine the influence on the magnetic properties of the R-metal sublayers in three-layer films.

Based on the data presented in Fig. 4, one can judge about the influence of the thickness of Co and Fe films and their thermal treatment on the shape of the hysteresis loops and the value of the residual magnetization and coercive force. Let us note some regularities of the obtained results.

Firstly, the pronounced dimensional dependence is not observed for Co and Fe films in the unannealed state and after thermal treatment, although the maximum value of the coercive force takes place at relatively small thicknesses. In all the cases, except the as-deposited Co films, the value of the residual magnetization increases with the film thickness.

Secondly, thermal treatment of Fe films leads to the fact that the hysteresis loops become wider with the simultaneous decrease in the residual magnetization that can be connected with partial oxidation processes in Fe films flowing at high-temperature annealing. Influence of the thermal annealing on the value of H_c is less expressed in Co films, although in whole it increases.

3.3 Multilayer film structures

Magnetic properties of three-layer Fe/Gd/Fe/Sub films in general are determined by ferromagnetic properties of Fe layers and magnetic ordering on the Fe/Gd interface and also depend on the thicknesses of Fe layer and intermediate Gd layer.

Analysis of the data illustrated in Fig. 5a shows the following. For the film samples with the thickness of Gd layer, which is in the crystalline state, $d > 10$ nm, the typical bend appears on the hysteresis loops. Such result can be connected with local remagnetization in Fe layers which are separated by a rather thick crystalline Gd layer. If effective thickness of Gd layer $d < 10$ nm, then hysteresis loop has the same shape as single-layer Fe film. The value of H_c also depends on the thickness and structural and phase state of Gd sublayer. For the films with quasi-amorphous Gd sublayer, the behavior of the dependence of the coercive force on its effective thickness has an oscillating character; the same tendency is also observed for H_c, which is defined from the data of magnetoresistive measurements and for magnetoresistance as well [9]. Such trend is typical for film nanocrystalline samples [18].

In the case, when Gd layer has crystalline structure with the increase in the thickness ($d_{Gd} > 10$ nm), the value of the coercive force increases. In contrast to H_c, the value of the residual magnetization decreases with the increase in the Gd layer thickness, for example, for Fe(5)/Gd(1)/Fe(20)/Sub, Fe(5)/Gd(20)/Fe(20)/Sub films it is equal to $M_r = 1.31 \cdot 10^6$ A/m, $0.93 \cdot 10^6$ A/m, respectively.

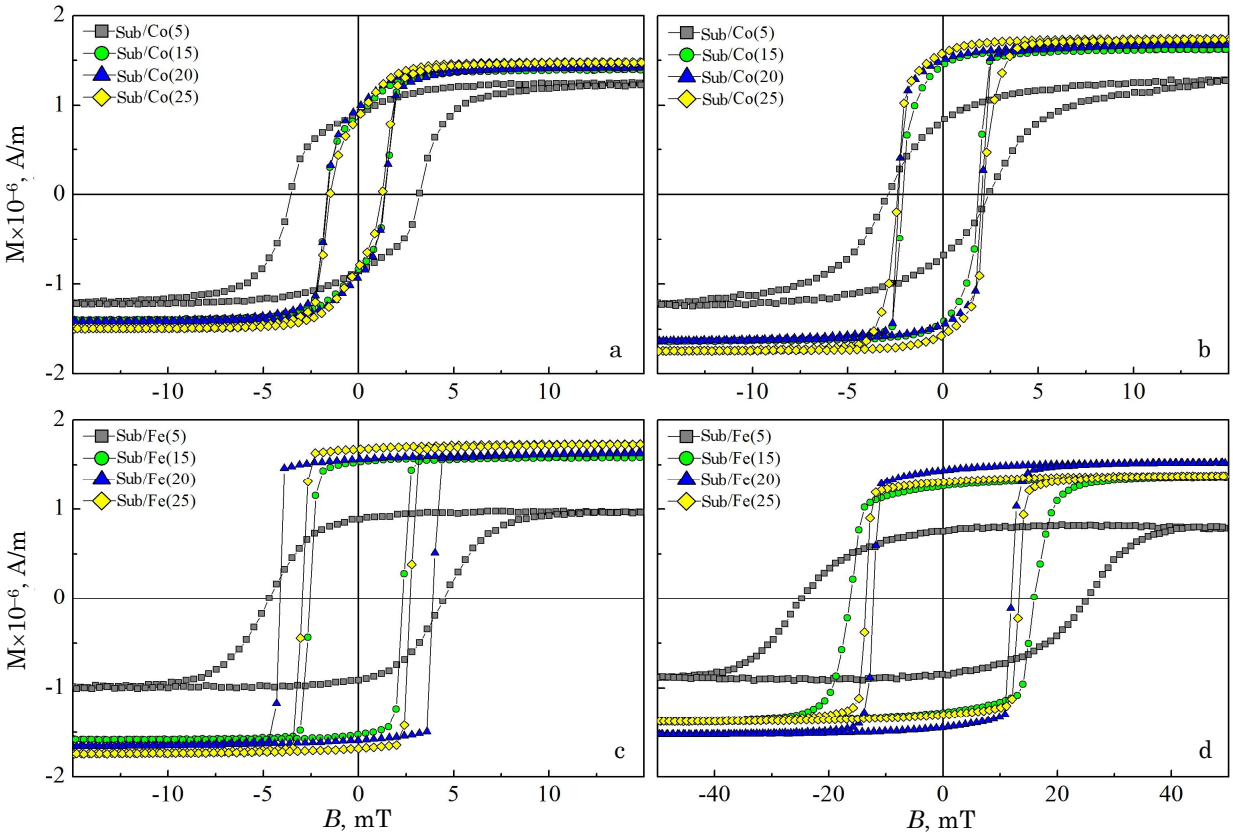

Fig. 4 – Dependence of the magnetization on the applied external magnetic field for monolayer Co (a, b) and Fe (c, d) films before (a, c) and after thermal treatment to T_a = 800 K (b) and T_a = 700 K (d), respectively

If compare coercivity of the systems with the total thickness of Fe layers with the same as the thickness of a monolayer film, one can note the following. The value of the coercive force in Fe films is higher in comparison with the systems where quasi-amorphous Gd acts as a sublayer. For the systems with crystalline Gd sublayer the coercive force has larger value. The above described trends remain in the films which were thermally treated. Annealing leads to the increase in the coercivity and decrease in the residual magnetization. At that, annealing to the temperatures T_a = 900 K induces, on average, a 5-fold increase in H_c in comparison with the as-deposited samples. Such result is connected with the oxidation processes in Fe layers. It is also necessary to pay attention to the shape of the hysteresis loops in the film samples which were thermally treated (Fig. 5b). As follows from the data, the forward and backward branches of magnetization curves do not overlap one another. Moreover, the higher annealing temperature is, the later forward and backward branches begin to coincide. Such result can be connected with blurring of the Fe/Gd interfaces due to the diffusion of Gd atoms into Fe layer. Obviously, iron crystals will be more saturated with Gd atoms near the layer interface than from the opposite side. Coercivity in such crystals increases relative to the Fe crystals. This conclusion agrees with the data of the work [19], where alloys based on R/T metal are studied and it was shown that they have higher coercivity in comparison with the samples, in which individuality of the layers remains. Thus, diffusion processes near the interface influence the magnetic properties of Fe/Gd/Fe three-layer film systems.

Differences in the influence of quasi-amorphous or crystalline Gd or Dy phases on the magnetic properties of the whole system are also partially visible on the example of the samples with different thicknesses of Co, Gd and Dy layers. Typical bends (Fig. 6) on the hysteresis loops, which are connected with remagnetization of Co layers of different thickness, although they are less expressed than in Fe/Gd/Fe/Sub films, are also manifested at relatively large thicknesses of intermediate layers based on crystalline Gd and Dy.

The value of the coercive force of the film systems with the total thickness of Co layers, which is the same as the thickness of single-layer Co film, has less value. An oscillating behavior of the dependence of H_c on the effective Gd thickness is exhibited for Co/Gd/Co/Sub systems in as-deposited state and after thermal treatment. While for Co/Dy/Co/Sub systems the value of H_c increases with the growth of the Gd thickness. In the case of both systems, the value of the residual magnetization decreases with the increase in the thickness of R metal.

Magnetic properties of three-layer Co/Gd(Dy)/Co/Sub film systems have their own features connected with the changes of the magnetic properties of Co layers during the polymorphous transition hcp → fcc, which is accompanied by the increase in the coercivity (Fig. 6c,d). The processes, which also take place in Fe/Gd/Fe films, are typical for the mentioned systems after annealing, i.e. the backward and forward branches of the magnetization curves do not overlap each other that can be connected with the flowing of the diffusion processes.

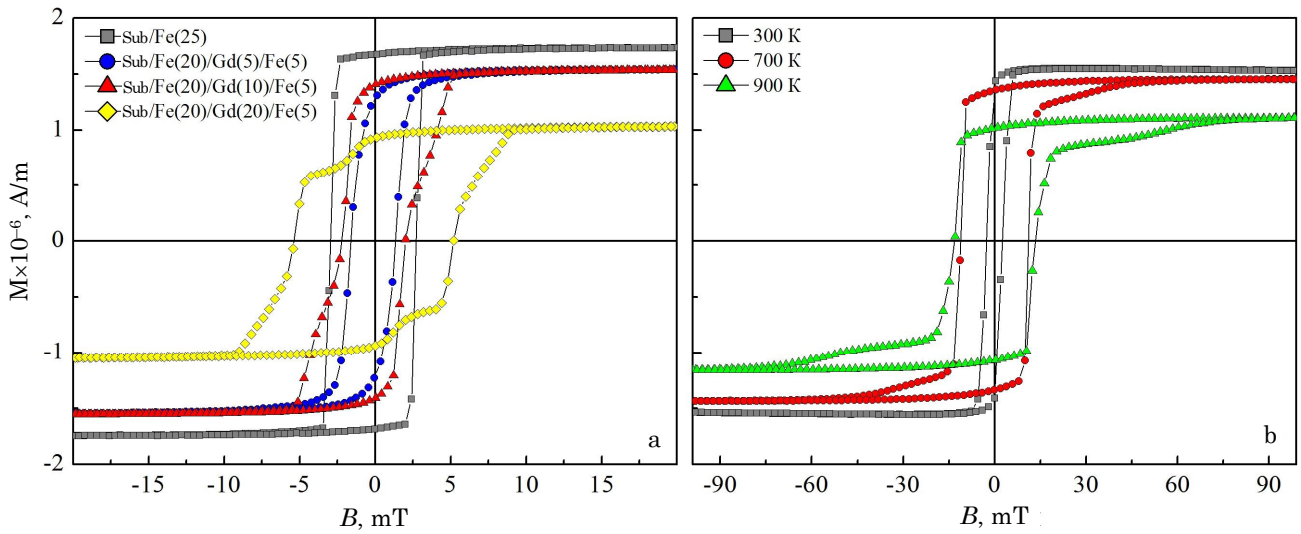

Fig. 5 – Dependences of the magnetization on the applied external magnetic field for monolayer Fe film and Fe/Gd/Fe/Sub three-layer film systems in as-deposited state (a) and for Fe(5)/Gd(10)/Fe(20)/Sub system before and after thermal treatment to the temperatures of T_a = 700 K and 900 K (b)

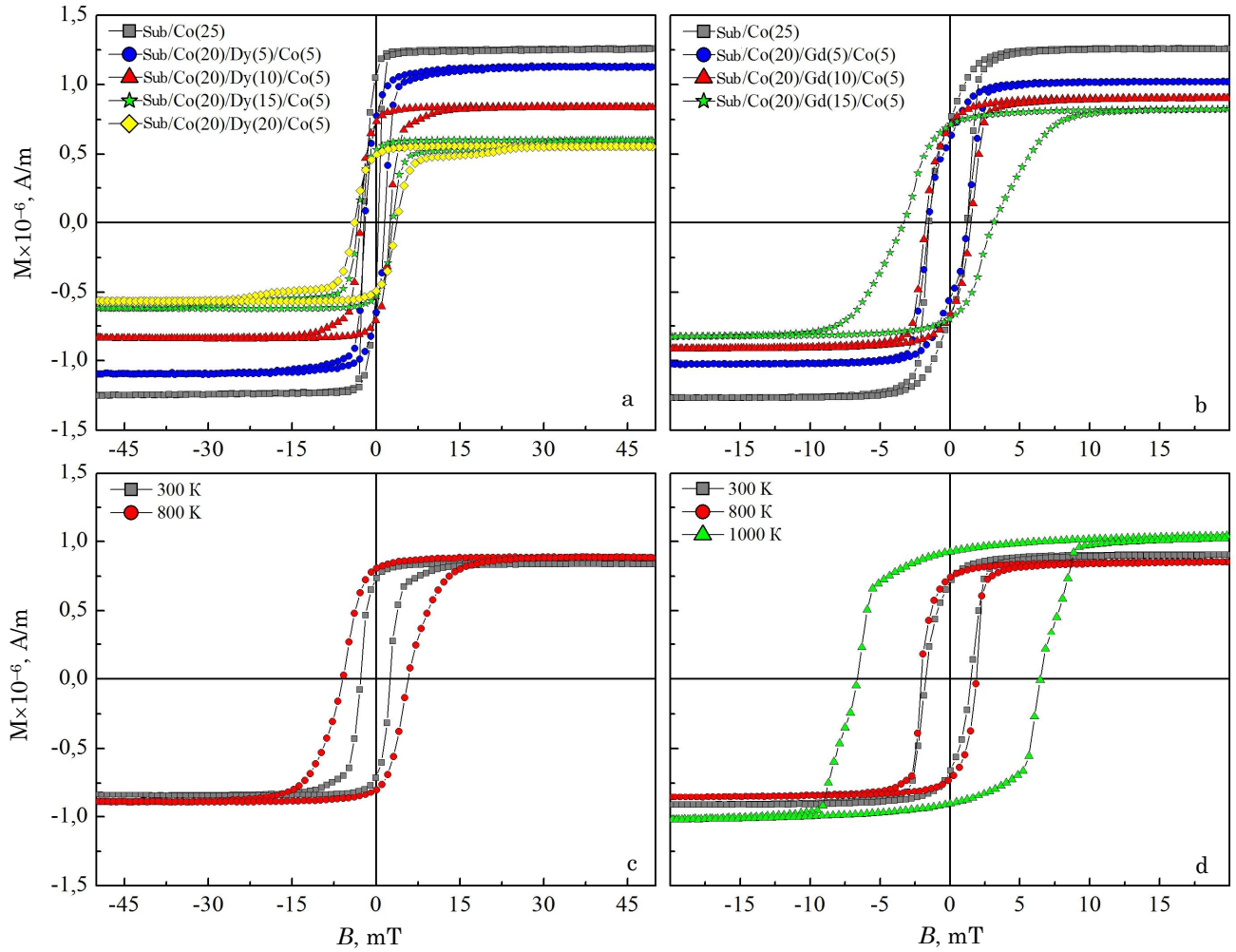

Fig. 6 – Dependences of the magnetization on the applied external magnetic field for monolayer Co film and Co/Dy/Co/Sub (a) and Co/Gd/Co/Sub (b) three-layer film systems in as-deposited state and for Co(5)/Dy(10)/Co(20)/Sub (c) and Co(5)/Gd(10)/Co(20)/Sub (d) systems before and after thermal treatment to T_a = 800 K and 1000 K

4. CONCLUSIONS

Based on the results of the presented investigations one can conclude the following:

1. Quasi-amorphous phase is fixed on the electron diffraction patterns of monolayer Gd and Dy films at their effective thicknesses less than 10 nm; and with the increase in the thickness from 10 to 40nm the crystallization processes become apparent, in particular,

– Gd films in as-deposited state have phase composition hcp-Gd + fcc-GdH_2 with bcc-Gd_2O_3 traces;

– phase composition of monolayer Dy films corresponds to hcp-Dy + bcc-Dy_2O_3;

– thermal treatment to T_a = 800 and 1000 K does not significantly influence the change of phase composition, although the increase in the oxide phase is observed.

2. Phase composition of Co(Fe)/Gd(Dy)/Co(Fe)/S three-layer films does not substantially differ from the phase composition of single-layer films, system components, excluding composition of sublayer based on Gd, in which in as-deposited state bcc-Gd_2O_3 oxide phase is not fixed on the electron diffraction patterns; it starts to appear only after annealing higher than T_a = 800 K.

3. Investigation of the magnetic properties of monolayer Co and Fe films and three-layer systems has shown their certain correlation with the structural and phase composition, in particular:

– the pronounced dimensional dependence of the coercive force on the thickness is not observed in monolayer Co and Fe films in as-deposited state and after thermal treatment;

– typical bends which imply layer-by-layer remagnetization of the layers are observed on the dependences of the magnetization on the applied external magnetic field for the effective thicknesses of Gd or Dy sublayers more than 15 nm;

– coercive force is larger for the systems with crystalline Gd or Dy sublayer than with quasi-amorphous one;

– thermal annealing in the majority of the cases leads to the increase in the coercive force;

– for three-layer films after annealing the following fact is typical: forward and backward branches of the magnetization curves do not overlap each other that can be connected with blurring of the interfaces because of the flowing of the diffusion processes.

AKNOWLEDGEMENTS

The authors of the paper express their gratitude for the possibility to conduct investigations to the workers of the Laboratory of magnetism of the University of Lorraine (Nancy, France).

This work has been performed under the financial support of the Ministry of Education and Science of Ukraine (Project No 0112U004688) and the Program of studying and training for students, Ph.D. students and professor's stuff abroad (2012-2013, University of Lorraine, Nancy, France).

REFERENCES

1. H. Nagura, K. Takanashi, S. Mitani, K. Saito, T. Shima, *J. Magn. Magn. Mater.* **240**, 183 (2002).
2. C. Bellouard, B. George, G. Marchal, N. Maloufi, J. Eugene, *J. Magn. Magn. Mater.* **165**, 312 (1997).
3. Y. Choi, D. Haskel, R.E. Camley, D.R. Lee, J.C. Lang, G. Srajer, J.S. Jiang, and S.D. Bader, *Phys. Rev. B.* **70**, 134420 (2004).
4. D. Haskel, G. Srajer, J.C. Lang, J. Pollmann, C.S. Nelson, J.S. Jiang, S.D. Bader, *Phys Rev. Let.* **87**, 207201 (2001).
5. K.V. Tyschenko, L.V. Odnodvorets, I.Yu. Protsenko, *Metallofizika i Noveishie Tekhnologii,* **33**, 10, 1351 (2011).
6. I.P. Buryk, D.V. Velykodnyi, L.V. Odnodvorets, I.Yu. Protsenko, O.P. Tkach, *Tech. Phys.* **81**, 2, 75 (2011).
7. T. Stobiecki, M. Czapkiewicz, M. Kopcewicz, *J. Magn. Magn. Mater.* **140-144**, 535 (2003).
8. N. Sato, K. Habu, *J. Appl. Phys.* **61**, 4287 (1987).
9. S.I. Vorobiov, I.V. Cheshko, A.M. Chornous, I.O. Shpetnyi, *Metallofiz. i Noveishie Tekhnol.* **35** No12, 1645 (2013).
10. *Diagrammy sostoyaniya dvojnyh metallicheskih sistem. Tom 2* (Red. N.P. Lyakisheva) (M.: Mashinostroenie: 1997).
11. Powder Diffraction Data File, The Joint Committee on Powder Diffaction Standards, International Center for Diffraction Data, Card No. 7429-91-6, p. 559 (1956).
12. M. Jergel, I. Cheshko, Y. Halahovets, P. Siffalovic, I. Matko, R. Senderak, S. Protsenko, E. Majkova, S. Luby, *J. Phys. D: Appl. Phys.* **42**, 135406 (2009).
13. S.I. Vorobiov, L.V. Odnodvorets, O.V. Pylypenko, A.M. Chornous, *Nanosys., nanomat., nanotekhnol.* **10** No4, 829 (2012).
14. S.S. Gorelik, L.I. Rastorguev, Yu.A. Skakov, *Rentgenograficheskiy i elektronno-opticheskiy analiz. Prilozhenie* (M.: Metallurgiya: 1970).
15. I.E. Protsenko, M.D. Smolin, V.G. Shamonya, et al., *Metally* **2**, 171 (1985).
16. T.B. Gorbacheva, *Rentgenografiya tverdyh splavov* (M.: Metallurgiya: 1985).
17. H. Kockar, T. Meydan, *J. Magn. Magn. Mater.* **242-245**, 183 (2002).
18. A.V. Svalov, V.O. Vas'kovskiy, K.G. Balymov, A.N. Sorokin, G.V. Kurlyandskaya, *Tech. Phys.* **59**, 530 (2014).
19. M. Gottwald, M. Hehn, F. Montaigne, D. Lacour, G. Lengaigne, S. Suire, S. Mangin, *J. Appl. Phys.* **111**, 083904 (2012).